Dispersion of the nonlinear second-order optical susceptibility of organic systems

C. C. Teng and A. F. Garito
Department of Physics, University of Pennsylvania, Philadelphia, Pennsylvania 19104-3859
(Received 11 August 1983)

Dispersion experiments of the second-order nonlinear optical susceptibility are reported for two fundamentally important organic systems *p*-nitroaniline and 2-methyl-4-nitroaniline for which detailed quantum-mechanical calculations have been completed. The frequency-dependent measurements were performed by dc-induced second-harmonic generation in liquid solutions with the use of a tunable (0.2—2 μm) laser source by stimulated Raman scattering from hydrogen gas. Accounting for dipole-mediated interactions between the molecular sites and the surrounding solvent medium provides quite satisfactory agreement between the experimental and theoretical results, demonstrating that the origin of exceptional nonlinear optical responses of organic systems resides in special highly charge-correlated electron states.

I. INTRODUCTION

In recent years theoretical and experimental interest has centered on the nature of highly-charge-correlated π-electron states in organic and polymeric crystalline structures that are responsible for exceptional second-order nonlinear optical responses $\chi^{(2)}_{ijk}(-\omega_3;\omega_1,\omega_2)$, particularly as exhibited by second-harmonic generation (SHG) and linear electro-optic effect (LEO) properties. The case of 2-methyl-4-nitroaniline (MNA) serves as an important example.[1,2] Its molecular structure along with its parent *p*-nitroaniline (PNA) is shown in Fig. 1. MNA crystals possess SHG and LEO figures of merit 50 times those of common dielectric insulators such as potassium dihydrogen phosphate (KDP) and 200 times those of semiconductors such as gallium arsenide (GaAs).[3] A remarkable property of MNA is the primarily pure electronic origin of $\chi^{(2)}_{ijk}(-\omega_3;\omega_1,\omega_2)$ over the entire frequency range from dc to optical frequencies.[2]

Currently, these electronic excitations are viewed as occurring on sites weakly coupled to their neighbors in an accentric structure and providing macroscopic sources of nonlinear optical response through the on-site microscopic second-order nonlinear electronic susceptibility β_{ijk}. In the rigid lattice-gas approximation,

$$\chi^{(2)}(-\omega_3;\omega_1,\omega_2)=Nf^{\omega_3}f^{\omega_2}f^{\omega_1}\langle\beta_{ijk}(-\omega_3;\omega_1,\omega_2)\rangle ,$$

where N is the number of sites per unit volume and f represents local-field corrections, and β_{ijk} is evaluated over the crystallographic unit cell. Thus, unlike common dielectric insulators and semiconductors, the origin of the magnitude and dispersion of the macroscopic susceptibility $\chi^{(2)}$ is reduced to experimental and theoretical studies of the corresponding microscopic susceptibility β_{ijk} of single molecular units comprising the optically nonlinear organic solid.

Lalama and Garito[4] have represented a detailed theoretical analysis of β_{ijk} and its dispersion for several molecular structures including PNA. Their results show that unique features of highly asymmetric charge-correlated excited states of the π-electron structure principally determine the magnitude, sign, and dispersion of β_{ijk}. Similar theoretical results[5] have been obtained for the lower symmetry case of MNA. Importantly, there are no analog states in common dielectric insulators, or semiconductors.

The microscopic susceptibility β_{ijk} is experimentally determined by electric-field-induced second-harmonic generation (DCSHG) measurements of liquid solutions as shown by Levine and Bethea,[6] Oudar and Chemla,[7] and Singer and Garito.[8] The measured polarization at the second-harmonic frequency 2ω produced by applied fields at ω and zero is given by

$$P_1^{2\omega}=\Gamma_{1111}E_1^0E_1^{\omega}E_1^{\omega} , \quad (1)$$

with statistical averaging over the Boltzmann distribution of molecules and all laboratory fields having a common linear polarization. The term $\Gamma_{1111}E_1^0$ is the effective second-harmonic susceptibility of the liquid solution. When the ground-state dipole moment μ is aligned along the molecular x axis, Γ_{1111} is given by[6]

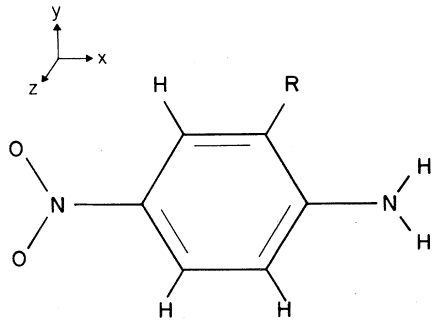

R = H ; CH_3

FIG. 1. Molecular structure of PNA ($R = H$) and MNA ($R = CH_3$).

$$\Gamma_{1111}\equiv\Gamma_L=Nf^0(f^\omega)^2f^{2\omega}\left[\gamma+\frac{\beta_x\mu}{5k_BT}\right], \tag{2}$$

where γ is the microscopic third-order susceptibility, which is negligibly small for conjugated molecules $\gamma\ll\beta_x\mu/5k_BT$; β_x is the vector part of β_{ijk},

$$\beta_x=\beta_{xxx}+\tfrac{1}{3}(\beta_{xyy}+\beta_{xzz}+2\beta_{yyx}+2\beta_{zzx}) . \tag{3}$$

However, local-field effects and solution interactions can lead to widely differing values for β_{ijk}. For example, the single-frequency values reported for β_x of PNA in nonpolar *trans*-stilbene is 6.4×10^{-30} esu (Ref. 9) and in polar, strongly interacting methanol 34.5×10^{-30} esu.[7] By combined experimental studies of DCSHG, dielectric constant, index of refraction, and specific volume, Singer and Garito[8] developed an infinite dilution extrapolation method for β_{ijk} that accounts for local fields and minimizes solute-solute and solvent-solvent interactions. Theoretical gas-phase values of β_{ijk} can then be compared to infinite dilution values if solvent-induced shifts of the singlet-singlet electronic excitations of the measured system are included.[10]

Earlier, we had communicated the first results[10] for the measured frequency dependence of β_{ijk} of PNA. In this paper we report the results of our completed DCSHG studies of the frequency dependence of β_{ijk} of PNA and MNA. The paper is arranged as follows. Section II summarizes the theoretical procedure for calculating β_{ijk}; Sec. III describes the tunable dye laser and stimulated Raman-cell experimental configurations used in the DCSHG measurements of the frequency-dependent β_{ijk}; Sec. IV presents experimental results; and Sec. V contains a comparison between experiment and theory for β_{ijk} and an analysis of the effects on β_{ijk} of solvent-induced excitation shifts (solvatochromism).

II. THEORY

The quantum-field-theory treatment of $\beta_{ijk}(-2\omega,\omega,\omega)$ provides a convenient diagrammatic representation of the three-wave-mixing process as shown by the space-time diagrams in Fig. 2. A ground-state $|g\rangle$ molecule with

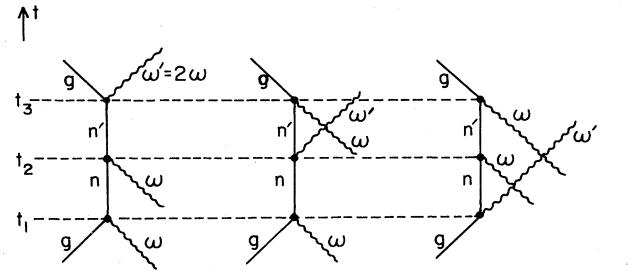

FIG. 2. Space-time diagram of the second-harmonic generation, where g represents the ground-state molecule, n,n' can be either ground or excited state.

eigenstates $|n\rangle$ and $|n'\rangle$ and eigenvalues $\hbar\omega_n$ in an electromagnetic field $\vec{E}^{\omega}(t)=\mathrm{Re}(\vec{E}^{\omega}e^{i\omega t})$ responds to the perturbing Hamiltonian $H'=e\vec{E}^{\omega}(t)\cdot\vec{r}$ in the dipole approximation that induces an electronic polarization in the molecular structure,

$$p_i^{2\omega}=\sum_{j,k}\beta_{ijk}(-2\omega;\omega,\omega)E_j^{\omega}E_k^{\omega} , \tag{4}$$

where $\beta_{ijk}(-2\omega;\omega,\omega)$ is the microscopic second-order nonlinear optical susceptibility, where both the fundamental and created combined frequencies are below electronic resonances but well above vibrational and rotational modes.

The quantized field is given by the expression

$$\vec{E}^{\omega}(t)=-\frac{1}{c}\frac{\partial\vec{A}}{\partial t}=-i\left[\frac{2\pi\hbar\omega}{V}\right]^{1/2}\sum_{\vec{k},\alpha}(a^{\dagger}_{k,\alpha}\hat{\epsilon}_{\alpha}e^{i\omega t}-a_{\vec{k},\alpha}\hat{\epsilon}_{\alpha}e^{-i\omega t}) , \tag{5}$$

where $a^{\dagger}$ (a) is the photon creation (annihilation) operator; $\hat{\epsilon}$, the polarization unit vector with $\alpha=1,2$; $\hat{k}$, the unit direction vector; and V, the normalization volume. The resulting quantum-field theory expression for β_{ijk} is[5]

$$\begin{aligned}\beta_{ijk}&=\tfrac{1}{2}(\beta_{ijk}+\beta_{ijk})\\&=-\frac{e^3}{4\hbar^2}\left\{\sum_{\substack{n\neq n',\\ n\neq g,\\ n'\neq g}}[(r^i_{gn'}r^j_{n'n}r^k_{ng}+r^i_{gn'}r^k_{n'n}r^j_{ng})(\omega_{ng}-\omega)^{-1}(\omega_{n'g}-2\omega)^{-1}+(r^j_{gn'}r^i_{n'n}r^k_{ng}+r^k_{gn'}r^i_{n'n}r^j_{ng})(\omega_{ng}-\omega)^{-1}(\omega_{n'g}+\omega)^{-1}\right.\\&\quad+(r^j_{gn'}r^k_{n'n}r^i_{ng}+r^k_{gn'}r^j_{n'n}r^i_{ng})(\omega_{ng}+\omega)^{-1}(\omega_{n'g}+2\omega)^{-1}]\\&\quad\left.+2\sum_n[r^j_{gn}r^k_{gn}\Delta r^i_n(\omega^2_{ng}-4\omega^2)+r^i_{gn}(r^k_{gn}\Delta r^j_n+r^j_{gn}\Delta r^k_n)(\omega^2_{ng}+2\omega^2)](\omega^2_{ng}-\omega^2)^{-1}(\omega^2_{ng}-4\omega^2)^{-1}\right\},\end{aligned} \tag{6}$$

where summations are over the complete sets of eigenstates $\langle n|$ and $\langle n'|$ of the unperturbed system. The quantities such as r^i_{gn} and r^i_{nn} are matrix elements of the ith components of the dipole operator for the molecule between the unperturbed ground (g) and excited states (n and n') $r^i_{gn}=\langle g|r_i|n\rangle$, and between two excited states

$r_{nn'}=\langle n \mid r_i \mid n' \rangle$, respectively; $\Delta r_n^i = r_{nn}^i - r_{gg}^i$ is the difference between the excited- and ground-state dipole moments; ω is the frequency of the applied optical field; and $\omega_{ng}=\omega_n-\omega_g$ is the difference between the excited- and ground-state energies. The expression for β_{ijk} is identical to that obtained from time-dependent second-order perturbation theory.[11] The first summation is referred to as an indirect term for which $n \neq n'$, and the second summation a direct term for which $n=n'$.

Calculation of β_{ijk} and its dispersion requires knowledge of the complete set of eigenstates $|n\rangle$ and $|n'\rangle$ of the system. Lalama and Garito[4] have developed a self-consistent-field (SCF), molecular Hartree-Fock procedure, including configuration interactions (CI) for electron-electron correlations, for calculating the frequency-dependent β_{ijk} of π-electron structures. All valence electrons are included, and the calculation is guided by experiment through the following three-step procedure: (1) determination of the many-body electronic ground state of the molecular system as an antisymmetrized product of the one-electron eigenfunction solutions of the Hartree-Fock equation, with the use of an all-valence-electron semiempirical parametrization. The solutions are directly compared to gas-phase experimental photoemission results; (2) accounting for correlations by CI calculations to form the lowest energy excited states and transition dipole moments of the molecule. These results are verified by comparison of calculated energies and oscillator strengths with gas-phase singlet-singlet excitation spectra; and (3) evaluation of the molecular second-order susceptibility β_{ijk} through Eq. (6). The theoretical procedure has been successfully applied to several resonant benzene structures including PNA and MNA and directly tested for predictive ability with success in calculations of quinoid structures possessing classical alternating single- and double-bond structures.

III. EXPERIMENTAL METHODS

The DCSHG experimental methods and techniques[12] for determining the frequency dependence of β_{ijk} used in the present measurements have been further studied in detail, and the results are being reported separately. The new method is essentially based on extensive design and development of the wedge Maker fringe experiment described earlier.[8] A brief summary will be given here.

The DCSHG optical design capable of detecting harmonic conversion to 10^{-12}–10^{-14} is shown in Fig. 3. A tunable pulsed-dye laser (Quanta Ray) is used as a pump beam into a compressed hydrogen-gas cell, generating Stokes lines from simulated Raman scattering tunable from 0.2 to 2 μm. P_1–P_{10} are beam-guiding prisms, and P_3 selects the proper Stokes line and sends it through the slit S_2. P_5 splits the beam into a reference beam and sample beam. The reference beam (right) passes through a quartz crystal R to provide a reference second-harmonic signal that is detected by the broadband photomultiplier tube PMT_1. The sample beam (left) acts as the input beam for second-harmonic generation in the liquid sample that is positioned on the translational stage assembly T_1-T_4. The sample cell [Fig. 4(a)] consists of two wedge-

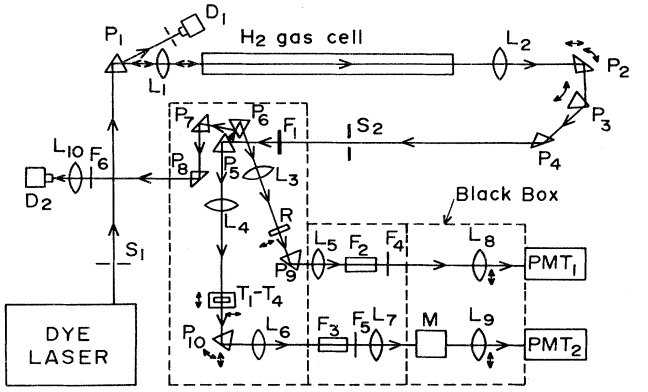

FIG. 3. Optical design for the DCSHG dispersion experiment, where the compressed H_2-gas medium was pumped by a tunable dye-laser source for Stokes generation by stimulated Raman scattering; P_1–P_{10}, beam-guiding prisms; P_3, Stokes-selecting prism; L_1–L_{10}, focusing lens; F_1–F_5, optical filters; M, monochromator; T_1-T_4, translational stages on which the sample cell is positioned; R, reference quartz crystal; and PMT_1, PMT_2 broadband photomultiplier tubes.

aligned optical glass windows (BK-7) positioned between two stainless-steel electrodes. The sample second-harmonic signal is detected by PMT_2. The ratio of the two outputs O_{PMT_2}/O_{PMT_1} is independent of the input beam power and therefore the effect caused by fluctuations in beam power is minimized. L_1–L_{10} are focusing lenses. F_4–F_6 are optical density filters. F_2,F_3 are frequency filters that block the fundamental beams, and F_1 filters out any optical noise which might mix with the harmonic signal. M is a monochromator. The photodiodes D_1 and D_2 trigger the gate electronics and monitor the beam power, respectively. A PDP 11/03 laboratory minicomputer controls the experiment and acquires and processes the data as previously described.

The intensity of the generated second-harmonic signal from the configuration shown in Fig. 4(b) is given by[13]

$$I_{2\omega}=AE_0^2 I_\omega^2 (T_1\Gamma_G l_c^G - T_2\Gamma_L l_c^L)^2 f(l) \tag{7}$$

with

$$f(l)=2\exp\left[-\left[\alpha_\omega+\frac{\alpha_{2\omega}}{2}\right]l\right] \times\left\{\cosh\left[\left[\alpha_\omega-\frac{\alpha_{2\omega}}{2}\right]l\right]-\cos\left[\frac{\pi l}{l_c^L}\right]\right\},$$

$$A=\frac{8\pi}{c}\left[\frac{8\omega}{c}\right]^2,\quad T_1=t_{2\omega}^G t_\omega^2 \frac{1}{n_{2\omega}^G+n_\omega^G}\frac{n_\omega^G+n_{2\omega}^L}{n_{2\omega}^G+n_{2\omega}^L},$$

$$T_2=t_{2\omega}^G t_\omega^2 t'^2_\omega \frac{1}{n_{2\omega}^L+n_\omega^L}\frac{n_\omega^L+n_{2\omega}^L}{n_{2\omega}^G+n_{2\omega}^L},$$

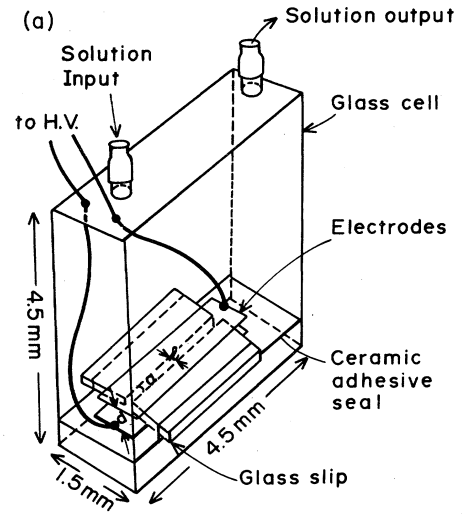

FIG. 4. Sample cell arrangement in the DCSHG experiment. (a) Structure, (b) side view and distribution of the static electric field E^0.

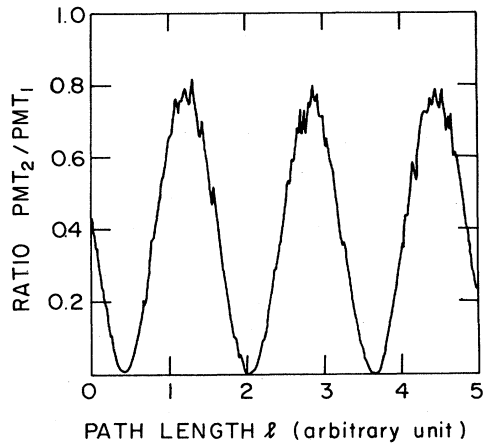

FIG. 5. Typical output fringes in the dc-induced second-harmonic generation experiment.

where

$$t_{2\omega}^{G}=\frac{2n_{2\omega}^{G}}{1+n_{2\omega}^{G}},\quad t_{\omega}=\frac{2}{1+n_{\omega}^{G}},\quad t_{\omega}'=\frac{2n_{\omega}^{G}}{n_{\omega}^{G}+n_{\omega}^{L}},$$

where E_0 is the applied dc electric field (in the liquid medium), I_ω is the fundamental beam intensity; n_ω^G (n_ω^L) the index of refraction of glass G (liquid sample L) at frequency ω; α_ω ($\alpha_{2\omega}$) is the absorption coefficient of the liquid sample at the fundamental (second-harmonic) frequency $\omega(2\omega)$; l is the sample optical path length; l_c^L (l_0^G) is the sample (glass) coherence length given by

$$l_c=\frac{\pi c}{2\omega(n_{2\omega}-n_\omega)} \tag{8}$$

and $E^0\Gamma_L$ ($E^0\Gamma_G$) is the effective dc-induced second-harmonic susceptibility of the liquid sample (glass).

The DCSHG measurements utilize several fixed fundamental wavelengths. The average input power levels are less than 0.3 mJ per 7-nsec pulse, well below the damage thresholds of glass and the liquid solutions. The Maker interference patterns are obtained by translating the sample cell along the y axis [Fig. 4(b)] at each wavelength as the sample second-harmonic signal versus pathlength l and exhibit standard behavior (Fig. 5) as expressed by Eq. (7). In the small absorptive-loss regime for both the fundamental and created second-harmonic beams, the Maker fringe data are analyzed using a least-squares-fit procedure to the function

$$y=A_1\sin^2\left[\frac{\pi l}{2A_3}+\frac{A_4}{2}\right]+A_2\ , \tag{9}$$

where (A_1+A_2) and A_2 are, respectively, the maximum and minimum of each measured fringe, A_3 is the coherence length l_c^L of the sample, and A_4 is the phase offset. The mean value of the fringes is given by

$$A_m=A_1/2+A_2\ . \tag{10}$$

Each measurement is repeated with a quartz reference crystal at the same position as the previously measured sample solution. This procedure allows Γ_L of the sample solution to be accurately determined relative to d_{11} of quartz (1.2×10^{-9} esu) (Ref. 14) through the expression

$$\frac{A_m^L}{A_m^Q}=\frac{E_0^2(T_1\Gamma_G l_c^G-T_2\Gamma_L l_c^L)^2(e^{-2\alpha_\omega \bar{l}}+e^{-\alpha_{2\omega}\bar{l}})}{(Q_1^2+Q_2^2)d_{11}^2(l_c^Q)^2}\ , \tag{11}$$

where $\bar{l}$ is the mean value of the sample optical path length,

$$Q_1=\frac{2n_{2\omega}^Q}{n_{2\omega}^Q+1}\frac{n_\omega^Q+1}{n_{2\omega}^Q+1}\frac{1}{n_{2\omega}^Q+n_\omega^Q}\left[\frac{2}{n_\omega^Q+1}\right]^2,$$

$$Q_2=\frac{n_{2\omega}^Q+n_\omega^Q}{n_{2\omega}^Q+1}\frac{1}{n_{2\omega}^Q+n_\omega^Q}\left[\frac{2}{n_\omega^Q+1}\right]^2.$$

For a two-component solution, Γ_L is the sum of the solvent (Γ_0) and solute (Γ_1) contributions expressed as

$$\Gamma_L=N_0 f_0^0(f_0^\omega)f^{2\omega}\gamma_0'+N_1 f_1^0(f_1^\omega)^2 f^{2\omega}\gamma_1'\ , \tag{12}$$

where for the ith constituent γ_i' is defined as $\beta_i\mu_i/5k_BT$ with β_i the microscopic second-order nonlinear optical susceptibility and μ_i the ground-state dipole moment. In order to minimize solvent-solvent and solute-solute interactions, Γ_L is determined as a function of solute concentration as weight fraction w and extrapolated to infinite dilution as previously described.[8] In the Onsager local-field formalism[8]

$$\frac{(2\epsilon_0+n_1^2)(2n_0^2+n_1^2)^3M_1}{(n_1^2+2)^4n_0^6\epsilon_0}\left\{v_0\left.\frac{\partial\Gamma_L}{\partial w}\right|_0+\Gamma_0\left.\frac{\partial v}{\partial w}\right|_0+v_0\Gamma_0-v_0\Gamma_0\left[\left.\frac{1}{n_0^2}\frac{\partial n^2}{\partial w}\right|_0+\left[\frac{1}{\epsilon_0}-\frac{2}{2\epsilon_0+n_0^2}\right]\left.\frac{\partial\epsilon}{\partial w}\right|_0\right]\right\}=N_A\gamma_1' , \tag{13}$$

where v is the specific volume, ϵ is the static dielectric constant, n is the index of refraction, N_A is Avogadro's number. The experimental time for sample and alternate reference runs did not exceed 10 min in order to avoid changes in beam profile due to heating effects in the laser source, which affects the readings of the harmonic signal. The accuracy of the measurement of Γ_L is 8% and is determined by uncertainties in the absolute values of the optical densities of the filters, the applied dc electric field, and day-to-day reproducibilities. The optical densities were measured separately with the use of a Perkin-Elmer Spectrophotometer model 330 at each frequency used in the DCSHG experiment, and applied dc electric field with the use of a Tektronix Oscilloscope model 466. The accuracy in the determination of the coherence lengths l_c^G and l_c^0 is only 1%. The actual day-to-day reproducibility of the Γ_L data is approximately 2% and is considered the best practicable measure of experimental uncertainty.

Measurements of the optical-absorption spectra of PNA and MNA were obtained using the Perkin-Elmer Spectrophotometer equipped with standard optical cells for gases and liquids. The absorption spectra were routinely analyzed with standard Gaussian curve-fitting procedures. PNA (Aldrich) was purified by multiple recrystallization followed by zone refining with 50 zone passes at a rate of 1 cm h^{-1}. The center zone was used. MNA (Aldrich) was purified by multiple recrystallization and two vacuum sublimations. Standard gas chromotograph and mass spectroscopy analyses established their chemical purity at greater than 99.995%. The solvent 1,4-dioxane (Burdick-Jackson) as received is triply distilled and standard precautionary procedures for solution preparation and handling were strictly followed to maintain dryness and avoid exposure to atmospheric humidity.

IV. RESULTS

The values of the nonlinear susceptibilities Γ_G and Γ_0 and the coherence lengths l_c^G and l_c^0 of BK-7 glass and pure dioxane, respectively, determined at different fundamental laser wavelengths are given in Table I. The uncertainty of each value is based on the actual reproducibility of the data for separate experimental runs. The frequency-dependent experimental values β_x^{expt} of the vector part of β_{ijk} for PNA and MNA are given in Tables II and III, respectively. In addition to experimental reproducibility of the data, the uncertainty of each β_x^{expt} value includes small deviations from linearity observed in plots of Γ_L versus weight fraction w, especially at higher frequencies where the quantity $(\partial\Gamma_L/\partial w)_0$ (Tables II and III) is sensitive to the approach of the created second harmonic to the PNA and MNA resonant excitation energies. This observation is further discussed below.

V. DISCUSSION

The extended theoretical analysis of β_{ijk} for several molecular structures showed that the detailed nature of

TABLE I. Frequency dependence of the measured Γ and l_c of glass (G) and pure 1,4-dioxane (0).

λ (μm)	$\hbar\omega$ (eV)	Γ_G (10^{-14} esu)	Γ_0	l_c^G (μm)	l_c^0 (μm)
1.907	0.650	3.45	4.50	39.12	105.7
		±0.03	±0.05	±0.04	±0.2
1.370	0.905	3.30	5.07	32.29	53.6
		±0.03	±0.02	±0.04	±0.2
1.060	1.170	3.20	5.3	20.56	26.4
		±0.05	±0.1	±0.03	±0.1
0.909	1.364	3.25	5.1	14.15	16.60
		±0.02	±0.1	±0.03	±0.03
0.830	1.494	3.12	5.1	11.03	12.50
		±0.02	±0.1	±0.04	±0.03

TABLE II. Frequency-dependent experimental values β_x^{expt} of PNA dissolved in 1,4-dioxane.

λ (μm)	$\hbar\omega$ (eV)	$\left.\frac{\partial\Gamma_L}{\partial w}\right\|_0$ (10^{-12} esu)	β_x^{expt} (10^{-30} esu)
1.907	0.650	6	9.6
		±0.3	±0.5
1.370	0.905	7.4	11.8
		±0.2	±0.3
1.060	1.170	10	16.9
		±0.3	±0.4
0.909	1.364	16	25
		±0.6	±1
0.830	1.494	24	40
		±2	±3

TABLE III. Frequency-dependent experimental values β_x^{expt} of MNA dissoloved in 1,4-dioxane.

λ (μm)	$\hbar\omega$ (eV)	$\left.\frac{\partial\Gamma_L}{\partial w}\right\|_0$ (10^{-12} esu)	β_x^{expt} (10^{-30} esu)
1.907	0.650	5.4	9.5
		±0.3	±0.5
1.370	0.905	7.3	12.8
		±0.3	±0.5
1.060	1.170	9.4	16.7
		±0.3	±0.5
0.909	1.364	15	27
		±0.6	±1
0.830	1.494	24	45
		±2	±4

charge correlations occurring in the π-electron excited states determines the magnitude, sign, and frequency dependence of β_{ijk}. For PNA,[4] of nine lowest energy singlet excited states with their associated oscillator strengths [4.20(0), 4.37(0.49), 4.38(0.01), 5.57(0.39), 6.14(0.09), 6.63(0.73), 6.80(0), 7.06(0.30), and 7.49(0) eV], the major contribution to β_{ijk} originates from virtual excitations to a unique highly charge-correlated second excited state $\hbar\omega_{2g}=4.37$ eV through the direct term of Eq. (6). This many-body excited state possesses relatively large values for both the transition moment $\mu_{2g}^x=-er_{2g}^x$ of 5.6 D and dipole-moment difference $\Delta\mu_2^x=-e\Delta r_2^x$ between the ground and excited states of 5.8 D.

In the lower symmetry case of MNA, recent calculations[5] show that among the lowest energy singlet excited states with their associated oscillator strengths [4.24(0.20), 4.25(0.04), 4.35(0.23), 5.46(0.45), 6.09(0.25), 6.51(0.58), 6.69(0), 7.02(0.27), and 7.52(0) eV], the first excited state $\hbar\omega_{1g}=4.24$ eV and the third $\hbar\omega_{3g}=4.35$ eV provide nearly equal dominant contributions to β_{ijk} through both the direct and indirect terms of Eq. (6). Again these unique π-electron excited states possess highly asymmetric charge-correlated behavior and associated large transition moments $\mu_{1g}^x=3.5$ D and $\mu_{3g}^x=3.6$ D and dipole-moment differences $\Delta\mu_1^x=2.3$ D and $\Delta\mu_3^x=3.4$ D.

From the DCSHG measurements of β_{ijk}, the frequency-dependent experimental values β_x^{expt} for PNA and MNA in dioxane [● in Figs. 6(a) and 6(b), respectively] increase smoothly as the fundamental frequency ω is increased and begin to diverge as 2ω approaches the excitation frequency ($\hbar\omega_{ng}\sim 3.5$ eV), which in each case corresponds to the first major optical excitation to the respective charge-correlated excited states of PNA, or MNA, dissolved in dioxane. For each system, the set of frequency-dependent experimental β_x^{expt} values is red-shifted to lower energies compared to the theoretical gas-phase dispersion curve [solid lines in Figs. 6(a) and 6(b)]. This difference between the experimental and theoretical dispersion results is due to solvent-induced (solvatochromic) shifts $\hbar\Delta\omega_{ng}$ to lower energies of the gas-phase singlet-singlet excitation energies. These shifts are easily

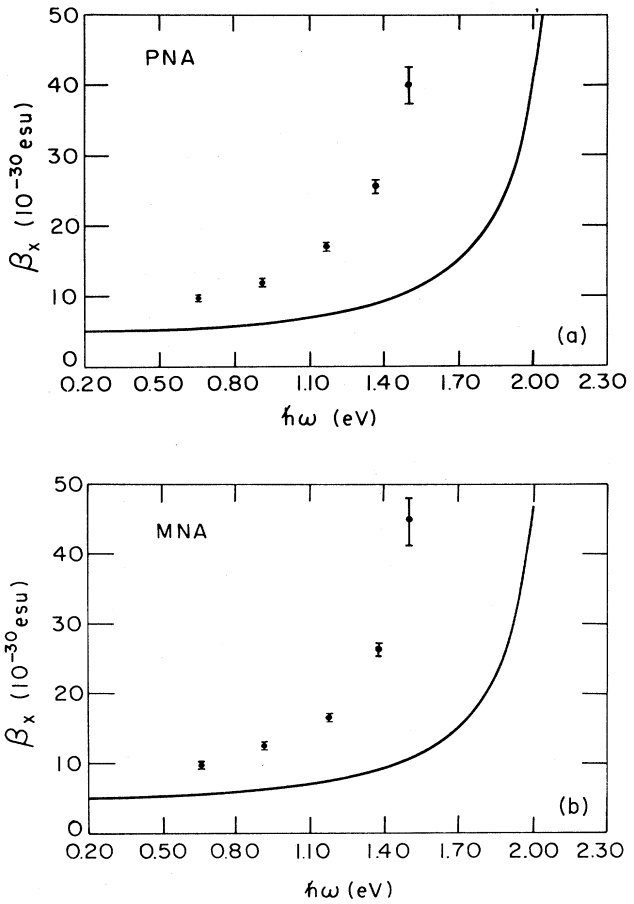

FIG. 6. Dispersion of β_x: ●, experimental points of the sample dissolved in 1,4 dioxane; ——, gas-phase theoretical calculation (a) PNA, (b) MNA.

observable in solution absorption spectra. The spectra for PNA and MNA measured in the gas phase and in dilute ($w=2\times10^{-5}$) dioxane solutions are compared in Figs. 7(a) and 7(b), respectively, showing the same frequency shift as observed in the β_x results.

It has long been known that solvent-induced shifts in $\pi\rightarrow\pi^*$ excitation energies are principally caused by dipole-mediated interactions that change the difference between the solute ground-state and excited-state dipole moments. These dipole interactions are standardly analyzed with perturbation theory and classical reaction field methods.[15] The shift in excitation energy $\hbar\Delta\omega_{ng}$ in the dipole approximation is given by

$$\hbar\Delta\omega_{ng}=A\,\Delta\mu_{ng}(\mu_n+\mu_g)+B\,\Delta\mu_{ng}\mu_g\ , \tag{14}$$

where

$$A\equiv\frac{1}{a^3}\frac{n^2-1}{2n^2+1}\ ,$$

$$B\equiv\frac{2}{a^3}\left[\frac{\epsilon-1}{2\epsilon+1}-\frac{n^2-1}{2n^2+1}\right]\ ,$$

with n the index of refraction of the solution; ϵ, the dielec-

tric constant of the solution; a, the effective cavity radius of the molecular site; μ_n and μ_g, the solute dipole moments for the excited and ground states, respectively. The first and second terms, respectively, are the reaction field experienced by the permanent dipole moment of the solute due to interaction with (1) the induced dipole moments of the surrounding molecules, and (2) the permanent dipole moments of the solvent and of other solute molecules at relatively high concentrations.

For nonpolar solvents such as dioxane, the first term is largest (98—99 %) and, in the second term, the solute contribution at relatively high concentration ($w \sim 4 \times 10^{-3}$, which is the average concentration used in the Γ_L measurements) remains small (1—2 %) while the solvent contribution vanishes.[16] The solvent-induced red shifts observed for both PNA and MNA in dioxane are in agreement with the theoretical results for each case, showing that the dipole moments μ_n of the charge-correlated excited states are larger in magnitude than the ground-state dipole moment μ_g.

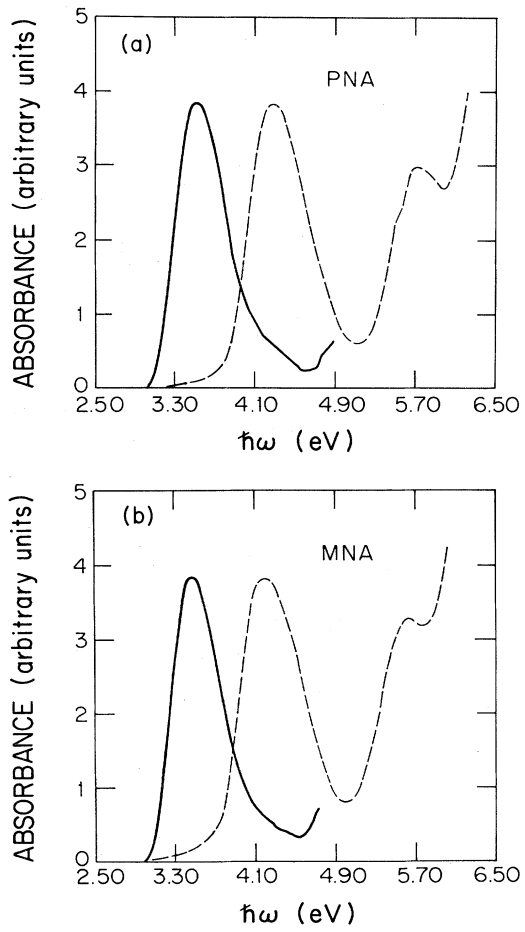

FIG. 7. Optical-absorption spectra of the sample dissolved in 1,4-dioxane (solid line) and in gas phase (dashed line) (a) PNA and (b) MNA.

The second term in Eq. (14) represents a refinement to the excited-state energy of approximately 2% referred to in our earlier reported[10] β_x^d values for PNA. In the DCSHG measurements the importance of this second smaller contribution was revealed by the observation that whereas the data points of Γ_L versus weight fraction w are linear at input beam frequencies away from the resonance region of the dispersion curve, positive deviations from linearity occur at higher weight fractions as the input beam frequencies approach the resonance region, where the quantity $(\partial \Gamma_L / \partial w)_0$ is much more sensitive to resonant excitation energies. To obtain $\hbar \Delta \omega_{ng}$ accurately in each case, the value of A was determined from the experimental optical-absorption spectra of dilute solutions and the value of B from the increased dielectric constant measured at the average concentration used in the Γ_L measurements. The new values for the state energies of the charge-correlated excited states are for PNA $\hbar \omega_{2g} = 3.46 \pm 0.01$ eV and for MNA $\hbar \omega_{1g} = 3.57 \pm 0.01$ and $\hbar \omega_{3g} = 3.30 \pm 0.01$ eV.

The SCF-CI calculations for the frequency-dependent β_{ijk} of PNA and MNA were repeated, using the new values for the state energies $\hbar \omega_{ng}$ in Eq. (6). The resulting theoretical dispersion curves for PNA and MNA are directly compared with the frequency-dependent experimental values β_x^{expt} in Figs. 8(a) and 8(b), respectively. Within experimental error, the agreement between experiment and theory is quite satisfactory. One can conclude therefore, that the microscopic electronic mechanism whereby virtual excitations to highly charge-correlated π-electron excited states result in exceptional second-order nonlinear optical responses is essentially correct and that the theoretical SCF-CI calculation represents suitable procedures for determining and analyzing the intrinsic β_{ijk} components. Moreover, in regard to experimental methodology, these results demonstrate that DCSHG liquid-solutions determinations of β_{ijk} must account for solvent-induced changes in the electronic excitations of the measured system. For π-π^* excitations, classical reaction field methods appear to adequately account for these solvent effects as dipole-mediated interactions.

In summary, the electronic excitations and interactions responsible for the frequency-dependent β_{ijk} as determined by DCSHG liquid-solution methods are suitably represented in perturbation theory to second order by the total Hamiltonian H

$$H = H_e + H_d + H_t \ ,$$

where H_e is the rigid lattice electron Hamiltonian used in the SCF-CI formalism, H_d is the dipole-dipole Hamiltonian identified with the reaction field method for solute-solvent interactions, and H_t is the Hamiltonian of the applied optical field in the electric-dipole approximation.

Finally, in this study of π-electron structures, we have shown that there is a direct relationship between the electronic second-order nonlinear optical response [Eq. (6)] and dipole-mediated solvent shifts [Eq. (14)] of optical excitations, or solvatochromism. Important to the emerging

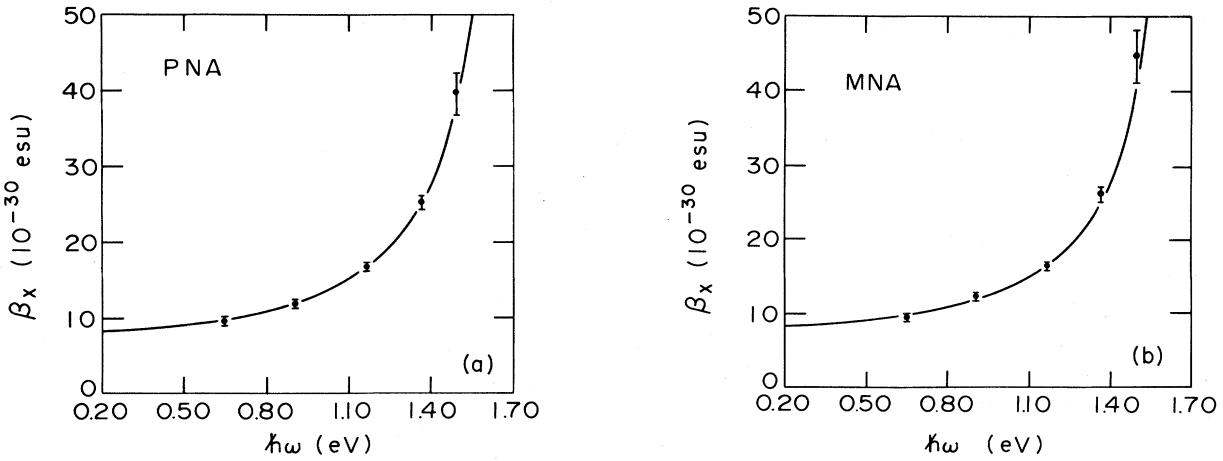

FIG. 8. Comparison between the experimental data points of frequency dependence of β_x (●) and the calculated results (——) accounting for solvent-shift effect. (a) PNA and (b) MNA.

field of molecular optics, which promises virtually limitless numbers of molecular structures, one can initially identify by simple independent measurements of the solvent shift $\hbar\Delta\omega_{ng}$ suitable structures possessing optically nonlinear responses optimized for experimental studies and a number of optical device configurations. These structures would include organics, charge-transfer salts, dyes, liquid crystals, polymers, and even organic transition-metal complexes. Results from additional studies of these relationships are being reported separately.

ACKNOWLEDGMENTS

This research was supported by the National Science Foundation Materials Research Laboratories Program under Grant No. DMR-79-23647 and by the U.S. Department of Defense Advanced Research Projects Agency under Grant No. DAAK-700-77-C-0045 (5-26502). We gratefully thank Dr. K. D. Singer, C. Grossman, and Dr. O. Zamani-Khamiri for many helpful discussions and Dr. A. McGhie for help in sample preparation.

[1]B. F. Levine, C. G. Bethea, C. D. Thurmond, R. T. Lynch, and J. L. Bernstein, J. Appl. Phys. 50, 2523 (1979).
[2]A. F. Garito and K. D. Singer, Laser Focus 18, 59 (1982).
[3]G. F. Lipscomb, A. F. Garito, and R. S. Narang, J. Chem. Phys. 75, 1509 (1981).
[4]S. L. Lalama and A. F. Garito, Phys. Rev. A 20, 1179 (1979).
[5]O. Zamani-Khamiri, A. F. Garito, and C. C. Teng (unpublished).
[6]B. F. Levine and C. G. Bethea, J. Chem. Phys. 63, 2666 (1975).
[7]J. L. Oudar and D. S. Chemla, J. Chem. Phys. 66, 2664 (1977).
[8]K. D. Singer and A. F. Garito, J. Chem. Phys. 75, 3572 (1981).
[9]B. F. Levine and C. G. Bethea, J. Chem. Phys. 69, 5240 (1978).
[10]C. C. Teng and A. F. Garito, Phys. Rev. Lett. 50, 350 (1983).
[11]J. F. Ward, Rev. Mod. Phys. 37, 1 (1965).
[12]C. G. Bethea, Appl. Opt. 14, 1447 (1975).
[13]J. L. Oudar, J. Chem. Phys. 67, 446 (1977).
[14]M. Choy and R. L. Byer, Phys. Rev. B 14, 1693 (1976). The variation of d_{11} over the working frequency range is only a few percent, according to Miller's rule.
[15]See, for example, A. T. Amos and B. L. Burrows, Adv. Quantum Chem. 7, 289 (1973) and references therein.
[16]For dioxane, the solvent molecules are slightly polar, and there are small contributions to the second term of (14) from the solvent. However, for the convenience of determining constants A and B, we include these minor contributions to the first term of (14) with negligible error.